

Article

Intercomparison Study of the Impact of Climate Change on Renewable Energy Indicators on the Mediterranean Islands

Alba de la Vara ^{1,2,*}, Claudia Gutiérrez ¹, Juan Jesús González-Alemán ³ and Miguel Ángel Gaertner ⁴

¹ Instituto de Ciencias Ambientales, Universidad de Castilla-La Mancha, Avda. Carlos III s/n, 45071 Toledo, Spain; claudia.gutierrez@uclm.es

² Departamento de Matemática Aplicada a la Ingeniería Industrial, E.T.S.I. Industriales, Universidad Politécnica de Madrid, 28006 Madrid, Spain

³ Departamento de Física de la Tierra y Astrofísica, Universidad Complutense de Madrid, 28040 Madrid, Spain; juanjego@ucm.es

⁴ Facultad de Ciencias Ambientales y Bioquímica, Universidad de Castilla-La Mancha, Avda. Carlos III s/n, 45071 Toledo, Spain; miguel.gaertner@uclm.es

* Correspondence: adelavaraf@gmail.com

Received: 28 August 2020; Accepted: 23 September 2020; Published: 27 September 2020



Abstract: The enhanced vulnerability of insular regions to climate change has been recently recognized by the European Union, which highlights the importance of undertaking adaptation and mitigation strategies according to the specific singularities of the islands. In general, islands are highly dependent on energy imports which, in turn, feature a marked seasonal demand. Efforts to reduce greenhouse gas emissions in these regions can therefore fulfill a twofold objective: (i) to increase the renewable energy share for global decarbonization and (ii) to reduce the external energy dependence for isolated (or interconnected) systems in which this can only be achieved with an increase of the renewable energy share. However, the increase in renewable technologies makes energy generation more dependent on future climate and its variability. The main aim of this study is to analyze future projections of wind and photovoltaic potential, as well as energy productivity droughts, on the main Euro-Mediterranean islands. Due to the limitations in land surface available in the islands for the installation of renewable energy capacity, the analysis is extended to offshore wind and photovoltaic energy, which may have an important role in the future increases of renewable energy share. To that end, we use climate variables from a series of simulations derived from Euro-CORDEX (Coordinated Downscaling Experiment) simulations for the RCP2.6 and RCP8.5 emission scenarios. A special effort is performed to normalize projected changes and the associated uncertainties. The obtained normalized changes make it easier the intercomparison between the results obtained in the different islands and constitute condensed and valuable information that aims to facilitate climate-related policy decision making for decarbonization and Blue Growth in the islands.

Keywords: Mediterranean islands; regional climate modeling; climate change; renewable energy; blue economy

1. Introduction

In a climate change context, the necessity of the implementation of adaptation and mitigation strategies is especially important in areas of enhanced vulnerability according to climate projections. The Mediterranean region has been identified as a particularly vulnerable area to climate change and is widely considered a climate hotspot since it gives an amplified climate signal [1]. This is exacerbated

in the Mediterranean islands, which are even more vulnerable due to their insular nature and external dependence on energy [2,3]. In this context, the European Commission declaration on clean energy [4] has put the focus on European islands as the next potential forerunners in the transition.

A high share of renewable energies in each country portfolio, together with an international diffusion of renewable energy innovations, is required to decrease GHG (i.e., greenhouse gas) emissions in the short term, e.g., [5,6]. Renewable energy deployment in islands has additional benefits. Many islands show a limited connection to the continent and most of them depend on energy imports [3]. Thus, the increase of local electricity from renewable energy sources favors energy independence from the outside and limits energy security issues [3]. In this context, it is important to take into account that an increase in the renewable energy share necessarily entails an increase in the dependence on the atmospheric variables and their variability—which can be subjected to changes in future climate. Currently, regional climate models (RCMs) are the most sophisticated tool available that can be used to project relevant climate variables in order to assess energy potential in future climate scenarios.

Different works have analyzed energy resources and potential for wind and photovoltaic (i.e., PV) energy over the Euro-Mediterranean area in the future using climate simulations [7–15]. In general, a certain increase is projected in wind potential in Northern Europe, in different emission scenarios, together with a reduction in the Mediterranean areas [8]. In the case of solar potential, a slight decrease is projected in the Mediterranean region by RCMs simulations [9,16]. However, models do not converge towards a single response in regions of Central Europe [15,17]. An important factor that could explain the observed discrepancies may be aerosol evolution, which is not considered in all climate simulations. While a robust ensemble of climate simulations including aerosol evolution would certainly improve estimations on photovoltaic potential, this is currently not available since model runs including aerosols are still scarce.

Many works have focused on the examination of energy potential changes [7–9,12,13,15]. However, all of them are focused on changes in energy potential over continental Europe and very little attention is given to insular regions. Given that the climate in these peripheral regions could be substantially different from that from the continental areas of the countries they belong to, and offshore energy sources can be more necessary for the islands due to land surface restrictions, different approaches may be required for the energy transition. Therefore, an individual resource evaluation is required. In order to properly capture land–sea gradients, as well as the orographic effect on climate variables, an enhanced horizontal model resolution is needed. Consequently, results obtained making use of global climate models (GCMs) [12,13], have an insufficient resolution to be used to address the Mediterranean islands. In this case, high-resolution regional simulations such as those from the Euro-CORDEX project [18] (i.e., horizontal resolution of 12 km) would allow for a more adequate characterization of climate variability in Mediterranean islands.

Because of the isolated nature of islands, the availability of marine resources is particularly important and promising due to the incipient deployment of offshore wind and solar technologies in the near future [19–25]. These two technologies represent, up to now, a maturity stage that makes them more suitable than other offshore and/or floating technologies which will be more developed in the coming years [26,27]. Offshore technologies are advantageous for islands or countries with limited space for the installation of power generation plants. In addition, wind resources are greater over the sea and, for solar panels, there is an increase in cell performance due to the cooling effect of water and wind on PV cells [28]. Despite some disadvantages that have to be overcome (corrosion problems due to salty water or the impact of waves on the installations), offshore PV is receiving growing interest, and has been already tested for a Mediterranean island (Malta) [24] or in sea areas characterized by high waves [23]. Previous works have analyzed the offshore wind resources over the Mediterranean area and their future projections [29,30], showing a general decrease in the central Mediterranean and an increase in the Aegean Sea and the Gulf of Lyons.

The aim of this work is to assess changes in a series of renewable energy indicators (both onshore and offshore), for the first time, focused on Mediterranean islands (see the considered islands and their

location in Figure A1 of Appendix A). We do the calculations for a control time period (1986–2005), different future time periods (2046–2065 and 2081–2100) and RCPs (Representative Concentration Pathways). In particular, we consider the RCP2.6, a stringent mitigation scenario, and the RCP8.5, which assumes high GHG emissions (see [31] for further details). To that end, we use climate variables from a set of high-resolution Euro-CORDEX simulations. The energy indicators considered here include solar and wind energy, which are presently (and probably in the future) the backbone of the deployment of renewable energies due to their technological maturity and low cost. Additionally, periods in which a deficit of solar or wind production occurs are also analyzed using a variability indicator to which we refer, following [32], as energy productivity droughts. These provide an estimate of productivity variability over time and offer relevant information for mitigation purposes, since in future decarbonization scenarios the frequency and duration of droughts will determine the required energy storage and backup sources. Energy indicators are computed for the islands and also over the marine areas adjacent to them. Ensemble mean projected changes, as well as the uncertainties associated with those changes, are normalized. This allows us to assign scores that are useful to perform a straightforward comparison of the results obtained for the different islands. In this work—conducted in the context of the SOCLIMPACT H2020 project (DownScaling CLimate ImPACTs; <https://soclimpact.net>)—we provide relevant information for decision-makers of the Mediterranean islands. We map and rank relevant indicators over land, but also over the sea, which is relevant for Blue Growth. The novelty of this work is based on several aspects. First, we exclusively focus on the study of the Mediterranean islands, instead of on continental Europe—as done in most of the previous studies that analyze renewable energy projections. Second, we make an intercomparison of a series of normalized energy indicators among islands in order to provide condensed insights regarding future changes in renewable productivity for policymakers and stakeholders. Third, most of the previous works are exclusively based on energy potential mean changes, whereas here we also make the effort to study variability changes through the analysis of energy productivity droughts. This article is structured as follows. In Section 2, the methodology is presented. In Section 3, the most relevant results are presented. The discussion and conclusions are offered in Section 4.

2. Methodology

In this work, we make use of variables from a set of Euro-CORDEX simulations to estimate changes in a series of renewable energy indicators in the Mediterranean islands (see [18] for an overview of the Euro-CORDEX modeling framework). The chosen models, as well as the domains considered for each region, are shown in Table 1. Renewable energy indicators studied are wind productivity, photovoltaic productivity and energy productivity droughts (see a summary in Table 2). Wind and solar productivity are defined as the normalized series of power generation potential, that is to say, the produced energy divided by the installed capacity, and is given in kWh/kW. Renewable energy indicators are computed for what we define as the control time period (1986–2005), as well as for the central and final stages of the 21st century (i.e., 2046–2065 and 2081–2100, respectively). Results presented in this work (with the exception of those dealing with the seasonal and interannual variability, where absolute results for each year are presented as time series), are calculated using the averages over the whole corresponding time period. To study future climate changes of renewable energy indicators we use data from simulations forced with the RCP2.6 and RCP8.5 emission scenarios.

Table 1. Simulations considered in this study. The domains for each region are: Balearic Islands (lon: 0° E, 5.2° E, lat: 38° N, 41.12° N); Crete (lon: 22° E, 28.24° E, lat: 34° N, 37.12° N); Cyprus (lon: 31° E, 36.2° E, lat: 34° N, 36.08° N); Corsica and Sardinia (lon: 7° E, 11.16° E, lat: 38° N, 44.24° N); Sicily and Malta: (lon: 11° E, 17.24° E, lat: 35° N, 39.16° N).

CMIP5	Euro-CORDEX
Institution/GCM	Institution/RCM
MPI/M-MPI-ESM-LR IPSL/IPSL-CM5A-MR CNRM-CERFACS/CNRM-CM5 MOHC/HadGEM2-ES	SMHI/RCA4

Table 2. Definition and units of the indicators presented in the manuscript.

Indicator	Definition	Units
Wind productivity	Wind energy production divided by a unit of installed capacity	kWh/kW
Solar productivity	Photovoltaic energy production divided by a unit of installed capacity	kWh/kW
Wind productivity droughts	Days in which daily wind productivity is lower than 0.5 times the average wind productivity computed over the 20-year control period (1986–2005)	% of days
Photovoltaic productivity droughts	Days in which daily solar productivity is lower than 0.5 times the average solar productivity calculated over the 20-year control period (1986–2005)	% of days

2.1. Selected Models

Euro-CORDEX comprises a large set of simulations, which makes it necessary to select a reduced set of simulations that are able to cover the uncertainty of climate change projections. When downscaling simulations with RCMs (i.e., regional climate models), the uncertainty associated with the selection of the driving GCM (global climate model) is generally larger than the uncertainty associated with other sources, like the RCMs [33]. Therefore, the selected simulations consist of one RCM (RCA4) nested in four different GCMs (HadGEM2-ES, CNRM-CM5, IPSL-CM5A-MR, MPI-ESM-LR). The GCMs selection is based on the results from [34]. The criteria used to select the reduced set of simulations are the following:

- The GCMs should have a good performance in present-climate conditions.
- The GCMs should have output data available for lateral boundary conditions of RCMs.
- The GCMs should have been specifically used for driving EURO-CORDEX RCMs.
- The spread of future temperature change and precipitation change (aggregated over Europe, by the end of the century) should be adequately covered. In practice, these four models encompass annual mean changes of +3.5 to +6 °C and from 0 to +0.2 mm/d.

2.2. Calculation of Energy Indicators

2.2.1. Wind Energy Productivity

The methodology followed to compute wind energy productivity is based on [7]. To that end, we first compute the wind speed near the surface (i.e., 10 m) making use of 6-hourly U10 and V10 wind components derived from the regional climate simulations. Then, we calculate the wind speed

at the turbine hub height (WH). This height is set to 100 m for wind energy over land and to 150 m over the sea. WH, is considered as the average of the wind speed at 6 h intervals. Once we calculate WH at the turbine hub height, we later calculate wind potential (W_{pot}). W_{pot} is computed as in [10], with a standard power curve for the wind turbine with cut-in wind velocity, $V_I = 3$ m/s; rated velocity, $V_R = 12$ m/s and cut-out velocity, $V_0 = 25$ m/s. The W_{pot} is then computed as follows:

$$W_{pot} = \begin{cases} 0 & \text{if } V < V_I & (1) \\ \frac{V^3 - V_I^3}{V_R^3 - V_I^3} & \text{if } V_I \leq V < V_R & (2) \\ 1 & \text{if } V_R \leq V < V_0 & (3) \\ 0 & \text{if } V \geq V_0 & (4) \end{cases}$$

Finally, wind productivity (W_{prod}) is calculated from the wind potential produced by the 6 h averaged wind, multiplied by the number of hours (6 h). Then, W_{prod} is the energy produced divided by a unit of power installed.

2.2.2. Photovoltaic Energy Productivity

In order to obtain photovoltaic (PV) productivity, daily surface solar radiation (SSR) and ambient temperature from the climate simulations are used as input variables for a parametric PV model. The PV modeling process is described in [35–37] and can be summarized as follows. First, incident solar radiation that reaches solar cells inside the panels is obtained through the decomposition of global solar irradiation and the transposition to the plane-of-array (POA). Second, the electrical performance of the photovoltaic system is modeled considering a typical PV installation in order to obtain daily PV productivity (PV_{prod}), which is defined as the energy produced divided by the unit of power installed. Characteristics of the general PV system are the same ones described in [36,37], where a detailed description of the methodology followed in this work is presented.

2.2.3. Energy Productivity Droughts

Photovoltaic and wind energy productivity droughts are calculated as an indicator of productivity steadiness in the islands of study. Renewable energy droughts can be regarded as low-productivity periods during which the daily productivity, previously computed as explained above, takes values below a low-productivity threshold. To systematically identify energy droughts, a Deficiency Index (DI) is computed following [32]. This is defined as follows:

$$DI(i,j) = 1 \text{ if } P(i,j) \leq Po(i,j) \quad (5)$$

$$DI(i,j) = 0 \text{ if } P(i,j) > Po(i,j) \quad (6)$$

where $P(i,j)$ is the daily productivity for each model cell (kWh/kW) and $Po(i,j)$ the corresponding low-productivity threshold. Although the definition of the DI is based on [32], in that work the authors do not calculate DI cell by cell, but consider spatial averages instead. Our approach, therefore, allows for a more realistic description of the spatial variability of energy productivity droughts. This low-productivity threshold permits us to characterize energy droughts [32] and is calculated as a percentage of the mean daily productivity estimated for the control time period. In particular, this threshold, following [32], is defined as 0.5 times the mean daily productivity estimated over the entire control period of study. According to the above expression, energy productivity droughts occur when the DI is equal to 1. A potential advantage of the energy productivity drought definition from [32] is that, as indicated by the authors, the DI does not depend on time or the electricity demand. Thresholds to determine productivity energy droughts in the scenarios are computed taking the mean daily productivity of the studied region for the control time period.

2.3. Normalization of Ensemble-Mean Changes and Uncertainties

A normalization of projected ensemble mean changes (i.e., mean obtained considering all simulations) and the corresponding uncertainties are implemented in order to provide scores that allow us to perform a straightforward intercomparison between the results obtained for the Mediterranean islands. Normalized values for projected ensemble mean changes for the selected energy indicators in the different regions, time periods and scenarios are given by the N_c index, which ranges between 0 and 1. A value of N_c of 0.5 indicates that changes are subtle. When $N_c > 0.5$, projected changes are not favorable, being $N_c = 1$ the worst scenario. This entails that productivity (droughts) decreases (increase). On the contrary, values of $N_c < 0.5$ indicate the opposite, being $N_c = 0$ the best scenario possible. The N_c index is defined as:

$$N_c = 0.25 \cdot A + 0.75 \cdot B \quad (7)$$

where the term A serves to quantify the projected ensemble mean change in a region in a relative way comparing it to the ensemble mean change projected for the rest of the islands and the term B allows us to evaluate the ensemble mean change projected for each island, time period and scenario in a relative way compared to the control period value, using a threshold of $\pm 10\%$ change. This threshold has been selected based on available studies on the impact of climate change on wind and PV energies, which show that the future projected changes frequently do not exceed a level of 10% relative to present values over the studied area [38–40].

Normalized uncertainties associated with ensemble mean projected changes for each island, scenario and time period are provided by N_u . In this case, values close to 0 indicate that the ensemble models predict similar changes, while values close to 1 correspond to the opposite case. We define the N_u index as follows:

$$N_u = C \cdot 0.5 + D \cdot 0.5 \quad (8)$$

where C represents the spread of projected changes predicted by the individual models that conform to the ensemble and D takes into account whether all models predict changes of the same sign, or not. A complete explanation regarding the calculation of N_c and N_u is provided in the Appendix A.

3. Results

In this section, we first present maps in which the regional ensemble mean spatial distribution of the different indicators is shown for each island and for the control time period. Then, ensemble mean absolute changes in the different islands and indicators are commented on. Later, results of the normalization of projected changes and the associated uncertainties for the different islands are presented. Additional insight into projected changes is given by the study of seasonal time series of selected islands.

3.1. Regional Distribution of Indicators in the Control Time Period

Figures 1 and 2 show the ensemble mean regional distribution of wind productivity, wind productivity droughts, solar productivity and solar productivity droughts in the control time period (i.e., 1986–2005). Overall, we observe that wind productivity is greater over the sea than over land. This may be related to reduced friction in marine areas due to the absence of obstacles and the higher altitude of the wind turbine considered for the offshore calculations. In line with this, wind productivity droughts are more frequent in areas where wind productivity is low and vice-versa. As to PV productivity we observe, on average, little contrast between land and sea. Notwithstanding, we note that it is clearly influenced by the existing orography. Specifically, it takes smaller values in highly elevated regions. This may be related to an increase of cloudiness over the most prominent mountain chains. Coherent with this, PV productivity droughts develop more frequently on top of the mountains. We also observe that, in general, PV droughts are much less frequent than wind droughts. This result found in the

Mediterranean islands studied is in line with findings from [32] for southern Europe. A more detailed description of the results obtained for the islands located in the Western and Central Mediterranean Sea, as well as for the islands placed in the Eastern Mediterranean, is given below.

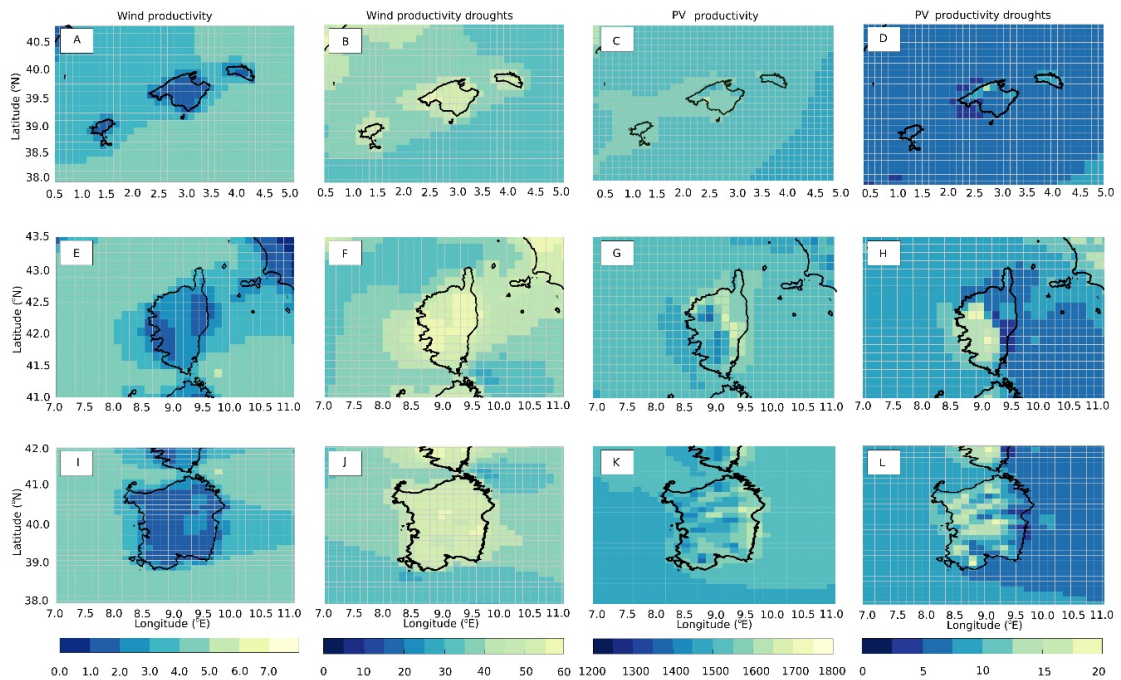


Figure 1. Ensemble mean wind productivity and frequency of wind productivity droughts (first and second columns), as well as ensemble mean photovoltaic (PV) productivity and PV productivity droughts (third and fourth columns) in the Balearic Islands (A–D), Corsica (E–H) and Sardinia (I–L) in the control time period (1986–2005). Wind productivity is given in kWh/kW times 10^3 , PV productivity is given in kWh/kW and the frequency of droughts in % of days within the 20-year period.

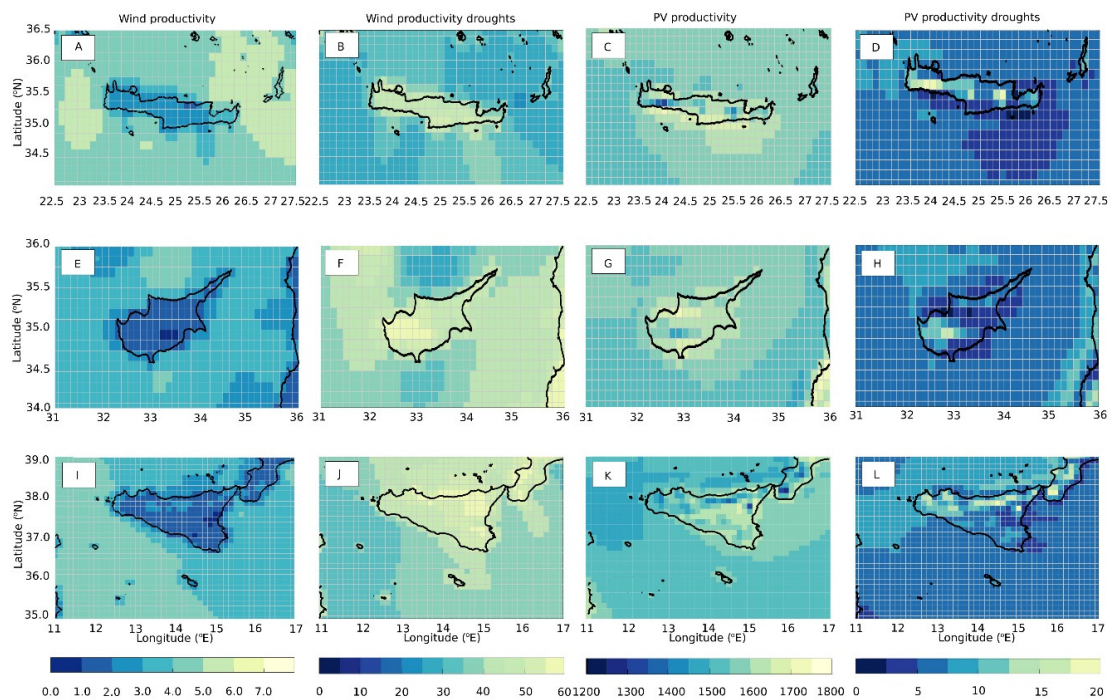


Figure 2. This is equivalent to Figure 1, but this has been created for Crete (A–D), Cyprus (E–H) and Sicily (I–L).

3.1.1. Islands from the Western and Central Mediterranean Sea

Balearic Islands

In the Balearic Islands region, wind productivity is greater to the E-SE of the model domain, over the sea, with values between 4000 and 5000 kWh/kW (Figure 1A). Wind productivity is lowest over land, with 1000–2000 kWh/kW. Wind productivity droughts develop with a frequency that varies between 30% and 60% of the days in this region (Figure 1B). Specifically, wind productivity droughts are less frequent to the E-SE of the model domain, coinciding with the region in which wind productivity is greater. Wind droughts are more frequent to the NW of Mallorca.

Different from wind productivity, PV productivity is generally greater over the land than over the sea, with values that range between 1500 and 1600 kWh/kW over Mallorca and Ibiza (Figure 1C). These values are in line with those provided by the Joint Research Center (JRC, https://re.jrc.ec.europa.eu/pvg_download/map_index.html) [41,42]. PV productivity features a visible minimum to the N of Mallorca, where the topography is abrupt. PV droughts are much less frequent than wind droughts. In this region, PV droughts only develop about 10% of the days (or less).

Corsica

In this region, wind productivity over land is modest, ranging between 1000 and 3000 kWh/kW. Minimum values of wind productivity are found to the NE and W of the island (Figure 1E). Wind energy potential is much higher over the sea, particularly north of the island and east of the Bonifacio Strait (marine passage between Corsica and Sardinia). Wind droughts are greatest over those areas in which wind productivity is smaller, where these develop from about 50 to 60% of the days (Figure 1F). From the islands located in the Western and Central Mediterranean Sea, Corsica is the one in which wind droughts are more prone to occur over land.

As to PV productivity, this attains a maximum close to 1700–1800 kWh/kW over those areas of the island in which topography is relatively low (Figure 1G). PV productivity decreases to values even smaller than 1400 kWh/kW along highly elevated mountain chains which extend to the central–western sector of the island from north to south. Regarding PV droughts we observe that, again, these occur less than 10% of the days, with the exception of highly elevated regions, where these are more frequent (Figure 1H).

Sardinia

In this area, wind productivity takes values between 3000 and 5000 kWh/kW over the sea and smaller values that range between 1000 and 3000 kWh/kW over land (Figure 1I). It is remarkable that the highest wind productivity values are found to the NE of the island, over the sea. This may be favored by topographic wind funneling. Regarding wind productivity droughts, these develop between 30 and 60% of the days over Sardinia (Figure 1J). The maximum frequency of wind droughts occurs over the island, with values that exceed 40–50%. These are less frequent between the southern coast of Sardinia and Africa, as well as to the east of the Bonifacio Strait, where topographic wind channeling occurs due to almost persistent westward winds [43].

PV productivity is greatest near the eastern coast of the island, reaching values close to 1700 kWh/kW (Figure 1K). In the rest of the island, PV productivity is lower. Minimum values between 1350 and 1450 kWh/kW are strongly influenced by topography as they develop in highly elevated areas. PV productivity droughts are, over land, clearly influenced by the existing topography (Figure 1L). On top of mountain chains, PV droughts increase their frequency to values close to 20%. Elsewhere in the studied domain, PV droughts develop with a smaller frequency, way below the frequency of wind energy droughts.

3.1.2. Islands from the Eastern and Central Mediterranean Sea

Crete

In Crete, wind productivity ranges between 2000 and 3000 kWh/kW approximately over land (Figure 2A). These are, by far, the highest values among all islands from the Eastern and Central Mediterranean Sea. Wind productivity is maximum in the marine areas immediately adjacent to the east and west of the island, reaching up to 5000–6000 kWh/kW, also larger than in marine areas around other islands. Wind productivity droughts develop around 40% of the days over the island of Crete (Figure 2B). In the marine areas around the island, regional changes in the frequency of wind droughts are lower and in line with the regional distribution of wind productivity.

As to PV productivity, the greatest values (greater than 1600 kWh/kW) arise over the island (Figure 2C). Notwithstanding, the topography causes minimum values from 1200 to 1400 kWh/kW localized on the top of the mountain ranges. As in other islands, PV droughts develop less than 10% of the days with the exception of elevated mountain chains, where these can be as frequent as 20% of the days (Figure 2D).

Cyprus

Wind productivity ranges between 1000 and 2000 kWh/kW over land, with lower values to the SE of the island (Figure 2E). In the marine areas adjacent to the north and south of Cyprus, respectively, wind productivity is greater than over the island. However, marine wind productivity is generally lower than in the sea areas around other islands. Regarding wind productivity droughts, these are relatively high all over most of the domain (Figure 2F). Wind productivity droughts increase to the SW of the island, near the mountainous region, with a frequency of droughts close to 60% of the days. Over the sea, wind droughts attain a magnitude of about 30% in the areas immediately to the north and the south of Cyprus.

PV productivity takes greater values over land than over the sea (values greater than 1600 kWh/kW), with the exception of the southern part of the island, where minimum values close to 1400 kWh/kW are found (Figure 2G). The decreased PV productivity is related, once more, to the presence of an abrupt topographic high. PV productivity droughts are generally less frequent than 10% of the days with the exception of the mountainous region to the north of the island, where PV droughts attain values close to 20% (Figure 2H).

Sicily and Malta

In the studied domain, wind productivity ranges between 3000 and 5000 kWh/kW over the sea, with the greater values towards the west (Figure 2I). In Sicily, productivity does not exceed about 3000 kWh/kW over land and the highest values are found to the north of the island. In Malta, productivity is slightly larger than in Sicily. Wind productivity droughts are more frequent over land and to the east of the studied domain, coinciding with the regions where wind productivity is smaller (Figure 2J). Wind droughts develop from 40 to 60% of the days in Sicily and Malta. The maximum frequency of wind droughts is found to the east of Sicily.

In Sicily, minimum values of PV productivity close to 1200 kWh/kW are found over the mountain chain located to the north of the island (Figure 2K). Coherently, PV productivity droughts occur around 10% of the days in the whole studied domain with the exception of the north of Sicily, where values greater than 10% are found (Figure 2L). Malta is an island with large restrictions on land-based renewable energy sources, due to its small size and large population density. Offshore wind energy has to overcome some problems, like deep bathymetry. Due to these limitations for Malta, offshore PV might be a relevant option to consider.

3.2. Ensemble-Mean Changes of Indicators in Different Islands, Time Periods and Scenarios

In general, changes of a greater magnitude are found for wind energy productivity in comparison to PV productivity (Figure 3A). Changes in wind productivity are not uniform within the Mediterranean islands. In the RCP2.6 scenario, positive changes for wind productivity (i.e., productivity increase) are found in Corsica, Sardinia and Crete over land and over the sea regardless of the time period considered, with the greatest increase in the Crete. In this scenario, absolute changes are, in general, of a smaller magnitude over land and for the end of the 21st century. A remarkable case is Cyprus, where positive changes occur for the RCP2.6 in the first half of the century and negative changes are projected for the end of the century over the islands and the marine areas adjacent to it. In the RCP8.5 scenario, Crete is the only region where wind productivity changes are positive. This is in agreement with previous studies in which positive changes over the Aegean Sea are projected [7,8,29,38–40]. Negative changes attain a greater magnitude in the RCP8.5 scenario, over the sea and by the end of the century.

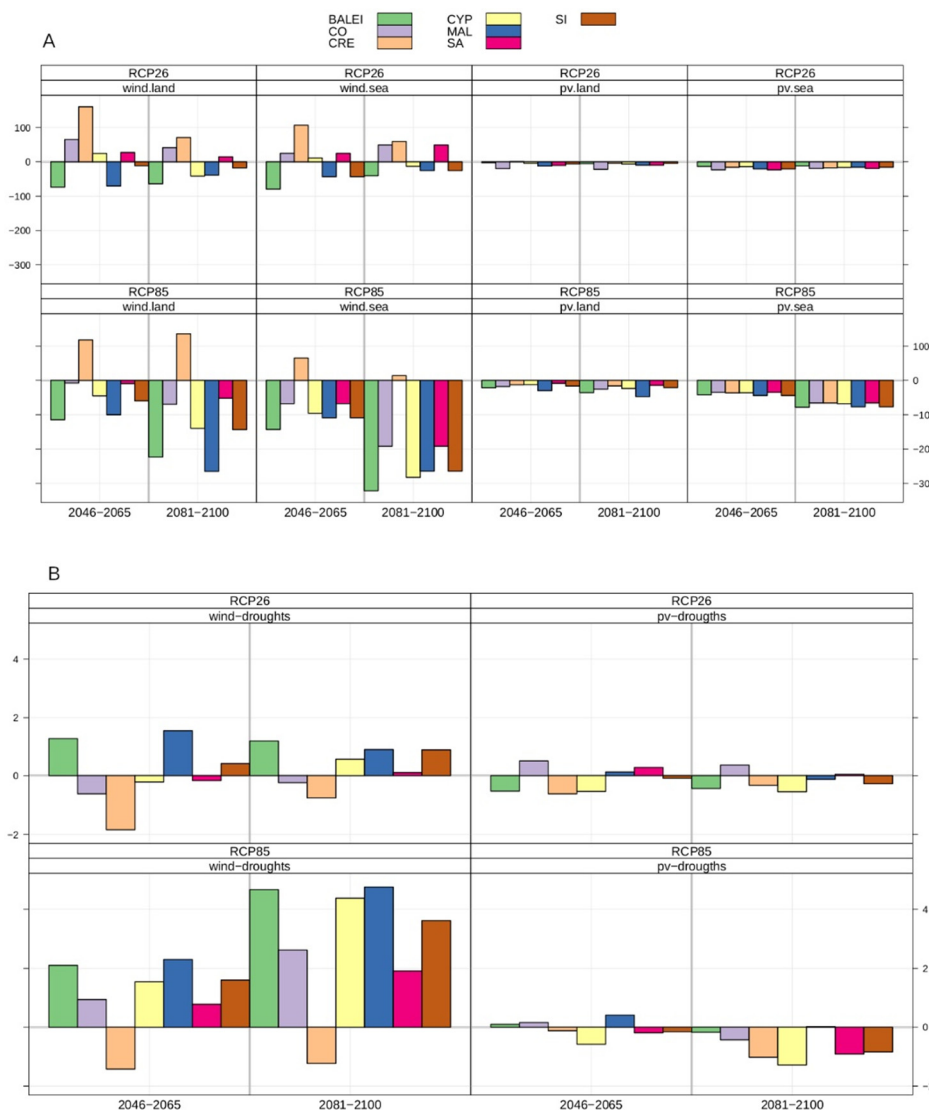


Figure 3. (A) Ensemble mean changes of annual wind (solar) productivity in absolute terms (kWh/kW) for the RCP2.6 and RCP8.5 scenarios and different periods over the sea and over the land. (B) Ensemble mean changes of annual wind (solar) productivity droughts in absolute terms (i.e., future minus control, in %) for RCP2.6 and RCP8.5 and the different periods. Each color represents an island/region (BALEI: Balearic Islands; CO: Corsica, CRE: Crete; CYP: Cyprus; MAL: Malta, SA: Sardinia, SI: Sicily).

In general, changes in the % wind productivity drought days are of a smaller magnitude in the RCP2.6 scenario than in the RCP8.5 case (Figure 3B). These notwithstanding, projected changes are, in absolute value, still small in the RCP8.5 scenario. Only wind droughts feature absolute changes above 4% in the Balearic Islands, Cyprus and Malta. These values are found in the RCP8.5 scenario by the end of the century. Observed changes in drought frequency are in agreement with variations observed in wind productivity. Thus, islands with a decrease in productivity show an increase in wind productivity droughts and vice-versa.

Productivity changes for PV potential show a homogeneous pattern regardless of the scenario. In particular, absolute values for the marine areas are greater than for land and greater values for the RCP8.5 scenario than for the RCP2.6. Negative changes are projected for PV productivity in all islands and the adjacent marine regions, time periods and scenarios. However, these changes represent a small percentage of the PV productivity of each region and are in line with the small changes projected for southern Europe in other studies [9,15]. Some authors have reported an increase in surface solar radiation and, as a consequence, an increase in PV productivity in the near future when RCMs include evolving aerosols [15,17]. The fact that models including aerosol evolution project a positive change in PV productivity means that, despite the uncertainty related to the direct effect of aerosols, this would reduce the risk of the worst-case scenario: a significant decrease in the solar resource.

In the RCP2.6 scenario, the Balearic Islands, Crete, Cyprus and Sicily experience a decrease in the frequency of PV productivity droughts and a slight increase for the rest of the islands for the first time period (2046–2065). For the second time period (2081–2100), only Sardinia and Corsica show a very small increase in the occurrence of PV droughts. In the RCP8.5 scenario, exclusively the Balearic Islands, Corsica and Malta present an increase in the frequency of PV droughts in the first period, while only Malta shows an increase in the second time period. Interestingly, despite the fact that a slight PV decrease is projected in all islands in terms of PV productivity, some regions also feature a decrease in the associated energy drought indicator. The fact that PV productivity and PV droughts do not present an inverse relation (i.e., a productivity increase associated with a decrease in the frequency of PV droughts and vice-versa) relates to the seasonality of the PV energy production. There is a clear annual cycle in PV energy production and most of the annual energy is produced in the summer months. Due to that, as energy droughts are calculated with respect to the annual mean, PV droughts occur mostly in winter months, showing an opposite annual cycle with respect to energy production. As a consequence, the seasonality of PV production changes affects productivity droughts that occur mostly in winter months.

3.3. Normalization of Projected Changes and Uncertainties

The aim of the normalization of projected changes (N_c) and the associated uncertainties (N_u) for the indicators is to provide a concise overview of the relative impacts of climate change on the different islands, offering a contrasting view to the absolute changes analyzed before. To obtain N_c , we do not only consider local changes in the islands, but also the magnitude of changes in comparison to the other islands. Thus, the values of N_c obtained for the different time periods and scenarios for the islands are easily comparable. Values of N_c and N_u for the different islands, time periods and scenarios are presented in Tables 3–8. N_c takes values that range from 0 to 1. Values close to 0 represent a positive change (i.e., relative increase of productivity or relative decrease of the frequency of productivity droughts), while values close to 1 indicate the opposite). When N_c is 0.5 future changes are subtle. N_u varies between 0 and 1, where 0 indicates that the ensemble members converge towards similar changes in the future (uncertainty is low) and 1 corresponds to the opposite case. In Tables 3–8, high uncertainty scores (N_u greater than 0.5) are indicated with an “*” and the specific values are presented in Appendix A.

Table 3. Normalized changes (Nc) for wind productivity for each island, scenario and time period. Deep green cells: Nc = 0–0.2; Light green: Nc = 0.3–0.4; White: Nc = 0.5; Light yellow: Nc = 0.6–0.7; Deep yellow: Nc = 0.8–1. Nc and Nu are computed over land. The * indicates the cases in which Nu > 0.5.

Wind Productivity (Land)		Balearic Islands	Corsica	Crete	Cyprus	Malta	Sardinia	Sicily
RCP2.6	2046–2065	0.8	0.3	0.1	0.4 *	0.7	0.4	0.5 *
	2081–2100	0.8	0.4 *	0.3	0.7	0.6 *	0.5	0.6 *
RCP8.5	2046–2065	0.9	0.5 *	0.2 *	0.7	0.7 *	0.5 *	0.7 *
	2081–2100	0.9	0.6 *	0.2 *	0.9 *	1.0	0.6 *	0.9

Table 4. As for Table 3, but for wind productivity over the sea. Domains considered for the calculations are shown in Table 1. The * indicates the cases in which Nu > 0.5.

Wind Productivity (Sea)		Balearic Islands	Corsica	Crete	Cyprus	Malta	Sardinia	Sicily
RCP2.6	2046–2065	0.7	0.4 *	0.3	0.5 *	0.6	0.4 *	0.6
	2081–2100	0.7	0.3	0.3	0.5 *	0.5 *	0.3	0.6 *
RCP8.5	2046–2065	0.8	0.6 *	0.3 *	0.7	0.7	0.6 *	0.7
	2081–2100	0.9	0.8	0.4 *	0.9 *	0.9	0.8	0.9

Table 5. Normalized changes (Nc) for wind productivity droughts for each island, scenario and time period. Deep green cells: Nc = 0–0.2; Light green: Nc = 0.3–0.4; White: Nc = 0.5; Light yellow: Nc = 0.6–0.7; Deep yellow: Nc = 0.8–1. Nc and Nu are computed over land. The * indicates the cases in which Nu > 0.5.

Wind Droughts		Balearic Islands	Corsica	Crete	Cyprus	Malta	Sardinia	Sicily
RCP2.6	2046–2065	0.7	0.4 *	0.2	0.5*	0.7	0.5	0.6 *
	2081–2100	0.7	0.4 *	0.3	0.6	0.7 *	0.5 *	0.7
RCP8.5	2046–2065	0.8	0.6	0.3 *	0.7	0.8	0.6	0.7
	2081–2100	1.0	0.7	0.3 *	0.9	1.0	0.7	0.9

Table 6. Normalized changes (Nc) for PV productivity for each island, scenario and time period. Deep green cells: Nc = 0–0.2; Light green: Nc = 0.3–0.4; White: Nc = 0.5; Light yellow: Nc = 0.6–0.7; Deep yellow: Nc = 0.8–1. Nc and Nu are computed over land. The * indicates the cases in which Nu > 0.5.

PV Productivity (Land)		Balearic Islands	Corsica	Crete	Cyprus	Malta	Sardinia	Sicily
RCP2.6	2046–2065	0.5 *	0.7	0.4 *	0.5*	0.6	0.6	0.5
	2081–2100	0.5 *	0.7 *	0.5 *	0.5	0.6 *	0.6 *	0.5 *
RCP8.5	2046–2065	0.6	0.6	0.6	0.6	0.7	0.6 *	0.6
	2081–2100	0.7	0.6	0.6 *	0.6	0.7	0.6	0.6

Table 7. As for Table 6, but this is constructed for PV productivity over the sea. Domains considered for the calculations are shown in Table 1.

PV Productivity (Sea)		Balearic Islands	Corsica	Crete	Cyprus	Malta	Sardinia	Sicily
RCP2.6	2046–2065	0.6	0.7	0.6	0.6	0.7	0.7	0.7
	2081–2100	0.6	0.6	0.6	0.6	0.6	0.7	0.6
RCP8.5	2046–2065	0.7	0.7	0.7	0.7	0.7	0.7	0.7
	2081–2100	0.8	0.8	0.8	0.7	0.8	0.8	0.8

Table 8. Normalized changes (Nc) for PV productivity droughts for each island, scenario and time period. Deep green cells: Nc = 0–0.2; Light green: Nc = 0.3–0.4; White: Nc = 0.5; Light yellow: Nc = 0.6–0.7; Deep yellow: Nc = 0.8–1. Nc and Nu are computed over land. The * indicates the cases in which Nu > 0.5.

PV Droughts		Balearic Islands	Corsica	Crete	Cyprus	Malta	Sardinia	Sicily
RCP2.6	2046–2065	0.1	0.8 *	0.1	0.1 *	0.6 *	0.7	0.4
	2081–2100	0.2 *	0.8 *	0.3	0.1	0.4 *	0.5 *	0.3 *
RCP8.5	2046–2065	0.6 *	0.6 *	0.4 *	0.0	0.8 *	0.4 *	0.4 *
	2081–2100	0.4 *	0.3	0.0 *	0.0	0.6 *	0.1	0.0

3.3.1. Wind Productivity and Wind Productivity Droughts

Regarding wind productivity over land, we observe that a general decrease is projected (with some exceptions) in the RCP8.5 scenario (Table 3). A more variable response, however, is found in the RCP2.6. In Corsica and Crete, Nc is very small. In Crete, Nc takes values smaller or equal 0.3 regardless of the scenario and time period considered. On this island, Nu is small in the RCP2.6 and is large in the RCP8.5. Nc is largest in the Balearic Islands, with values from 0.7 to 1 in each period and scenario and Nu smaller than 0.5. This points to an important (and solid) decrease in wind productivity—as seen in the previous section. Focusing on changes of wind productivity over the marine areas adjacent to the corresponding island(s), it is worth noting that similar insights to those extracted for land productivity are found (Table 4), but Nu generally takes now smaller values and thus results are less uncertain.

Values of Nc for wind productivity droughts (Table 5) show a good correspondence with those from wind productivity (Table 3). In particular, Nc takes values generally greater than 0.5 (with some exceptions). In the RCP8.5 scenario, all islands (except for Crete) present high values of Nc along with values of Nu lower than 0.5. Thus, a robust response from the models predicts a trustworthy increase in the frequency of wind productivity droughts in the majority of the Mediterranean islands. In the RCP2.6 scenario, values of Nc are more diverse and the uncertainty associated is larger. The sharpest increase in the occurrence of wind productivity droughts occurs, regardless of the scenario and time period considered, in the Balearic Islands. Furthermore, in this case, the associated uncertainty is low. Another interesting case is Crete, where normalized wind productivity droughts show a decrease (Nc values below 0.5) in occurrence, which is more robust for the RCP2.6 scenario.

3.3.2. PV Productivity and PV Productivity Droughts

Focusing on PV productivity over land we observe that, in the RCP2.6 scenario, in most regions (except for Corsica) changes are very small and Nc is close to 0.5 (Table 6). On the contrary, a clear increase of Nc is projected in all regions for the RCP8.5 scenario. In this case, the productivity decrease corresponds to Nc values that vary between 0.6 and 0.7 with low values of Nu. Interestingly, marine PV productivity shows in all time periods and scenarios, values of Nc between 0.6 and 0.8 (Table 7). In all cases, models converge towards a productivity decrease and Nu does not exceed 0.5 in any case, indicating a low overall uncertainty. Nc is higher in the RCP8.5 scenario, especially by the end of the 21st century.

Different from what has been found for PV productivity, normalized changes of PV productivity droughts are not similar for all regions, periods and scenarios (Table 8). Specifically, in the RCP2.6 scenario, the frequency of PV productivity droughts goes down and Nc is below 0.5 in both time periods for most of the islands, with some exceptions like Corsica. The values of Nc are strongly dependent on the island and chosen time period. In the RCP2.6 scenario, normalized values above 0.5 in both time periods are found in Corsica, with values of Nc greater than 0.7 but with high uncertainty. In the RCP8.5 scenario, Nc values below 0.5 of PV productivity droughts occur in both periods in Crete, Cyprus, Sardinia and Sicily. In the rest of the regions values of Nc are above or below 0.5 depending on the period.

3.4. Seasonal and Interannual Variability of Indicators: Study Cases

At this point, it is relevant to gain insight into the interannual and seasonal variability of the different indicators in the control, as well as in the future time periods. To that end, we examine the time series of the different indicators. This allows us to assess the impact of interannual and seasonal variability on the ensemble mean values and ensemble mean changes. We focus on two selected islands: Crete and Cyprus. Crete is chosen because of its anomalous behavior, which is not observed in the rest of the Mediterranean islands, i.e., wind productivity increases in all time periods and future climate scenarios and the frequency of wind productivity droughts goes down consistently. We consider also Cyprus, given that this is close to Crete (both are located in the Eastern Mediterranean), but this presents a behavior which is more representative of what observed in the rest of the Mediterranean islands, i.e., a wind productivity decrease and an increased frequency of wind productivity droughts in the future. In addition to this, interestingly, both PV productivity and PV productivity droughts show a decrease in the future. This, which is the case in most of the studied islands, is an interesting result to gain insight into. For brevity (and because results exhibit qualitatively the same patterns in the RCP2.6 and RCP8.5 scenarios), we construct the time series with results obtained for the RCP8.5 scenario. Furthermore, given that we aim to understand the climate signal and the surface area of these islands is not very large, averages to construct the time series are performed over the entire domain (see caption of Table 1).

3.4.1. Crete

Wind productivity presents a seasonal cycle which depicts only a subtle variability in the control time period (Figure 4A). Seasonal changes in wind productivity in Crete go in line with those reported in previous regional model studies [29,38,40]. This presents higher values in winter and summer, with a winter maximum close to 400–450 kWh/kW. In summer, wind productivity is higher than in spring and fall due to the reinforcement of the Etesian winds. The average increase of normalized wind productivity projected in RCP8.5 (Tables 3 and 4) relates to a wind productivity rise in summer and fall. It can also be noted that the amplitude of interannual variations is largest in winter and autumn, with variations of a similar amplitude in the control and the different future time periods considered.

Consistent with what stated in the previous paragraph, the seasonal pattern of wind productivity droughts (Figure 4B) features the minimum frequency of wind droughts in winter and summer (when wind productivity is greater) and the maximum frequency in spring and fall (with lower values of wind productivity). Accordingly, projected wind productivity droughts decrease in summer and autumn, this being responsible for the observed mean decrease shown in Table 5. The seasonal cycle of wind productivity and wind productivity droughts varies in opposite ways. This means that, overall, when wind productivity increases, the frequency of wind droughts goes down. Interannual variations in the frequency of wind droughts are, again, largest in winter and autumn. No clear difference in the amplitude of the interannual variations is found between the control and the future time periods studied.

PV productivity in the control period shows a distinct seasonal cycle, with maximum values above 140 (kWh/kW) in spring and summer, as well as minimum values below 100 (kWh/kW) in winter (Figure 4C). Regardless of the future time period chosen PV productivity remains roughly unchanged in winter, while this slightly decreases in spring, summer and fall. This entails that the average PV productivity decrease projected in this region (see Tables 6 and 7) is controlled by a reduction in spring, summer and fall. These seasonal changes have been observed by other authors [9,11–13] and are associated with an increase in temperature in southern Europe, which causes a reduction in cell efficiency. In all time periods, interannual variability is greater in winter than in the rest of the seasons, while summer months are more stable due to the anticyclonic situation.

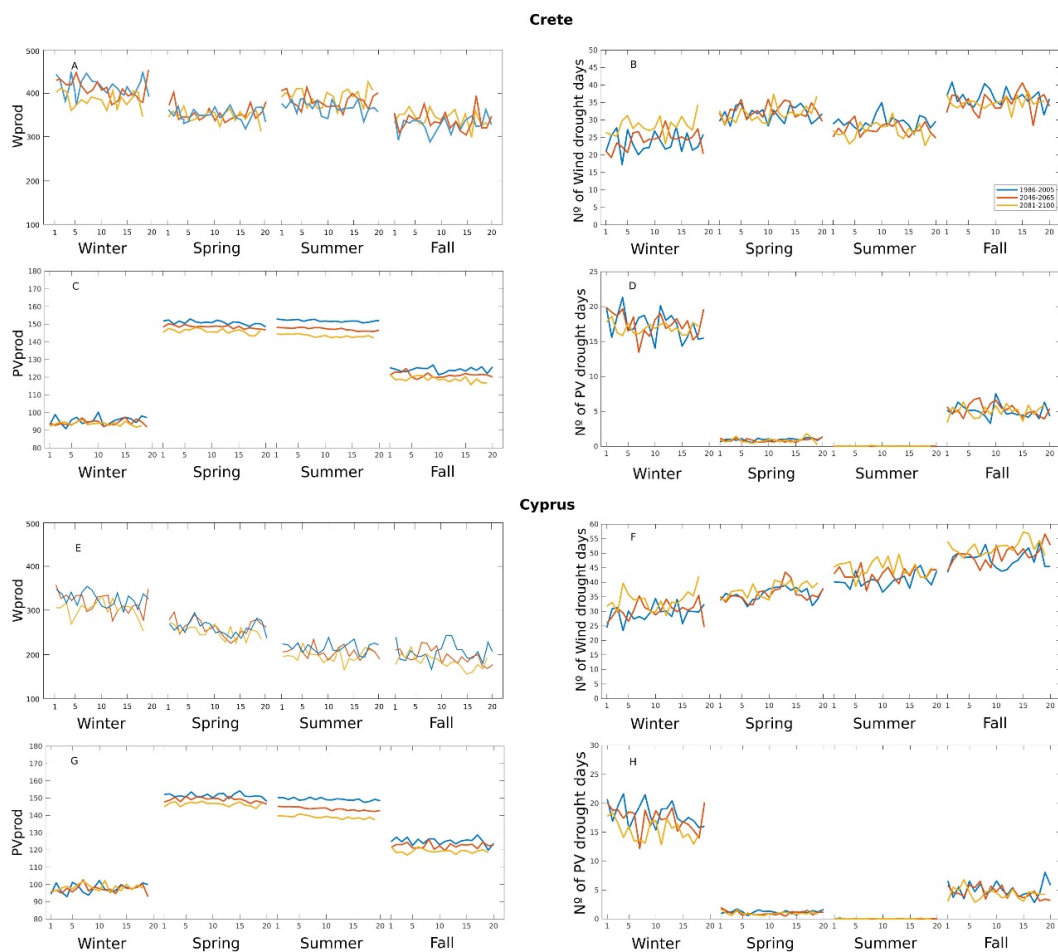


Figure 4. Seasonal time series for the different time periods, indicators computed for Crete (A–D) and Cyprus (E–H) for the RCP8.5 scenario. Depicted indicators are: wind productivity (A,E), wind productivity droughts (B,F), PV productivity (C,G) and PV productivity droughts (D,H). Productivity values are given in kWh/kW, in monthly average for each season, while productivity droughts are given in the number of drought days per season. In this figure, the control (1986–2005) appears in blue, the near-future period (2046–2065) in red and the distant-future period (2081–2100) in yellow.

In the control period, PV productivity droughts feature a marked seasonal cycle with a maximum in winter, a smaller frequency in fall and these are almost nonexistent in spring and summer (Figure 4D). The fact that PV droughts are almost absent in spring and summer indicates, once more, that insolation changes in winter and autumn largely determine the annual mean frequency of PV droughts. Therefore, the reduction of PV productivity observed in summer and spring (Tables 6 and 7), does not have an impact on the annual frequency of PV droughts (Table 8). Interannual variations of PV droughts are again, in all time periods, largest in fall and winter. Winter and fall productivity changes in the scenarios, relative to the control time period, are small, and so are changes in the frequency droughts.

3.4.2. Cyprus

The seasonal cycle of wind productivity in the control time period is different from that observed in Crete (Figure 4E). This is characterized by maximum values in winter, with a minimum in summer and fall. Results show that in the future—especially by the end of the 21st century—productivity drops in all seasons with respect to the control. Interannual variations of wind productivity are, regardless of the time period chosen, largest in winter.

Wind energy productivity droughts are more frequent than in Crete’s domain in the control time period (Figure 4F). Coherent with the wind productivity pattern, wind droughts are less likely to occur

in winter and more likely to develop in fall. In the future, wind productivity droughts increase in frequency in all seasons, particularly in the 2081–2100 period. Interannual variability displays a large variability in all seasons and time periods.

As to PV productivity, for the control time period, this displays qualitatively the same seasonal cycle as in Crete's domain (Figure 4G). This highlights the steadier nature of the seasonal cycle of solar productivity relative to that from the wind seasonal cycle, which is more influenced by local factors such as the surrounding topography. In the future, a slight decrease in PV productivity is observed in spring, summer and fall, especially by the end of the century. Winter months do not present important changes in future PV productivity. In all time periods, interannual variations are greatest in winter and fall.

PV productivity droughts present a similar seasonal pattern to that found for the Crete's domain in the control time period (Figure 4H). The fact that, qualitatively, the seasonal cycle of both islands studied in this section presents a similar shape indicates that PV productivity is on average less influenced by regional factors. Again, changes in the annual mean number of days with PV droughts are namely controlled by winter and fall insolation. The interannual variability is largest in fall and winter, especially in the latter. In winter, the number of drought days experiences a decrease which is particularly pronounced in the 2081–2100 time period.

4. Discussion and Conclusions

4.1. General Discussion

The strong need for increasing the contribution of renewable energy in the Mediterranean islands is being met presently to a very high degree through onshore wind and solar PV energy installations. This selection is supported by several reasons: the competitive and steadily decreasing price of energy from these mature technologies, the high potential in particular of PV energy over these islands, and the relatively low share of variable renewable energy sources in power production for most of them, which facilitates their integration in the power system. However, the need for very high renewable energy shares in the future and the possible impact of climate change on renewable energy resources are challenges that have to be tackled.

Regarding the latter issue, the future change of wind energy and PV productivity should be rather small in general: around 5% or less with respect to the reference period in many cases, with maximum changes of about 10% for some islands at the end of the century under RCP8.5 scenario (particularly for wind energy productivity over land). A 10% productivity change could have a significant impact on a planned or existing plant if it occurs over the lifetime of the power plant, but in this case, such a change would extend over many decades, which will facilitate adaptation and efficiency measures.

Wind and solar PV energy are not dispatchable, and its variability represents a challenge for its integration in the power system. This is a challenge that can be addressed through storage or backup plants (which can be itself renewable energy plants), through demand management, but also taking advantage of the complementarity of PV and wind energy and their very different variability characteristics. In this study, we have measured this variability through the frequency of renewable energy droughts. Solar PV, with drought frequencies of 10% or less of the days, is clearly more stable and reliable than wind energy, which shows drought frequencies of about 50% of the days for most islands. Additionally, solar PV and wind energy show usually a clear seasonal complementarity, as seen in the example of Cyprus analyzed here, which is characteristic for most islands. The implications of the higher stability of solar PV and its complementarity with wind energy are being recognized by stakeholders in the islands, as demonstrated by the report by Monitor Deloitte and Endesa [44], in which one of the key recommendations for achieving an accelerated zero carbon target in the Balearic Islands by 2040 is the combination of solar PV and wind energy, with clearly higher shares of PV than of wind energy. Our results show that projected changes in the frequency of droughts are small. This indicates that the time-variability characteristics of wind and PV energy are a robust feature.

Our analysis also includes offshore wind and solar PV technologies. The results confirm that offshore wind energy has a much higher potential in comparison to onshore wind energy. Even if future projections of offshore wind energy point also towards a limited decrease, the exploitation of this marine resource will imply in any case a large productivity improvement in comparison to land-based plants. Whereas offshore PV productivity does not show important differences in magnitude compared to land-based PV, offshore PV plants would be beneficial in small and/or densely-populated islands in which space is a limiting factor, such as Malta. In this respect, there is growing interest in offshore PV generation plants, as shown by the test plants being installed and the references made to this technology in the Roadmap for the Offshore Renewable Energy Strategy of the European Commission or in the report of [44] about the accelerated decarbonization of the Balearic Islands. This suggests that offshore technologies could play a relevant role in the pathway towards very high or 100% RES shares required to (i) achieve the long-term EU decarbonization strategy, (ii) decrease the external energy dependency of insular regions (i.e., reduce their vulnerability) and (iii) mitigate the effect of climate change on renewable energy generation.

The combination of different types of offshore renewable energy sources on the same platform is also attracting interest, as the different sources can exhibit complementarity in time and the combined output can be thus more stable and reliable. The different renewable energy technologies can also share part of the installations, like the connection to land, reducing their cost [45,46]. The European Union is trying to promote such combinations, through projects like MUSICA (Multiple Use of Space for Island Clean Autonomy), which will design and test a floating offshore platform integrating wind, PV and wave energy for use on islands and plans to develop roadmaps for its deployment in three case study islands, among them Malta [47].

Increasing RES shares together with a higher diversification of renewable technologies can limit the amount of power that needs to be imported to the islands through interconnections to the mainland. Interconnections are in principle very beneficial for supply safety, but excessive dependency on them should be nevertheless avoided, due to the risk of blackouts. The failure of a single element (one transmission line) can knock out instantaneously a large proportion of the power of an island and even cause an island-wide blackout, as has occurred several times in Malta in the last years.

4.2. Conclusions

In this work, we use high-resolution climate variables in order to compute a series of renewable energy indicators that allow us to assess the impact of climate change on renewable energy production, not only over the Mediterranean islands, but also over the marine areas adjacent to them, thereby encompassing a key aspect of the blue economy. In addition to wind and photovoltaic (PV) productivity, we also consider wind and PV productivity droughts, which are a measure of the variability of the resource.

Results for the control time period show a large spatial heterogeneity of wind energy productivity, with much larger values over the sea than over the islands. The maximum wind energy potential is found over Crete, which shows an atypical seasonal distribution with high summer values due to regional wind flow, and the Etesians. Solar PV productivity is spatially much more homogeneous, and is generally high in all the studied islands. Minimum values of PV potential are found in mountainous areas likely due to orographic-related cloud formation. The seasonal cycle of PV is always driven by an increase of solar irradiation in the central months of the year and presents little differences among regions.

Wind energy droughts are much more frequent (around 50% of the days for most islands) than PV droughts (10% or less of the days). This agrees with results from the study of [32], and highlights the much more stable nature of PV productivity in comparison to wind productivity.

The future projections of the impact of climate change show that adaptation needs in the area of renewable energies will be rather limited. The future change of wind energy and PV productivity should be rather small in general, with maximum changes at the end of the century under the

high-emissions RCP8.5 scenario. In general, projections show a decreasing trend of wind energy productivity, with a more important decrease in the RCP8.5 scenario. The main exception is Crete, which shows a consistent increasing tendency. Projected PV productivity changes are generally smaller than wind energy changes and, in most cases, PV productivity remains constant or slightly decreases.

Wind energy and PV productivity droughts will undergo generally rather small future changes. The sign of the changes in the frequency of wind energy droughts is linked to the sign of the productivity change, such that a productivity decrease (as obtained for most islands) is associated with an increase in the frequency of droughts. This is not found for PV productivity and droughts, which decrease simultaneously in several cases. This is due to the fact that the sharpest decrease in PV productivity occurs in summer and autumn when PV droughts do not develop. Therefore, even an annual mean decrease in PV productivity could drive a decrease in the frequency of PV droughts, as long as PV productivity increases in winter months.

The normalization of the changes and the associated uncertainties of the corresponding energy indicators provide condensed information that facilitates the intercomparison of the results obtained in the different islands. Combined with the use of an appropriate color code, tables of normalized scores provide a useful and direct way to communicate the impact of climate change on RES in the islands to policymakers and stakeholders.

There is a specific uncertainty source in PV projections over Europe. Most regional climate model simulations, including the ones used here, do not include a projected evolution of aerosols in future climate runs. The missed effect of the likely evolution of aerosols may increase to some degree the future surface solar radiation and PV productivity over most of the islands [15]. This could cancel out the limited reduction of PV productivity obtained in the present study. Thus, a similar analysis to the one we perform, but done with RCMs simulations including evolving aerosols, could constitute an interesting follow-up when a large set of RCMs including aerosol evolution is available.

Author Contributions: Conceptualization, A.d.I.V., C.G., J.J.G.-A. and M.Á.G.; methodology, A.d.I.V., C.G., J.J.G.-A. and M.Á.G.; formal analysis, A.d.I.V., C.G., J.J.G.-A.; investigation, A.d.I.V., C.G., J.J.G.-A. and M.Á.G.; resources, A.d.I.V., C.G., J.J.G.-A.; data curation, A.d.I.V., C.G., J.J.G.-A.; writing—original draft preparation, A.d.I.V. and C.G.; writing—review and editing, A.d.I.V., C.G., J.J.G.-A. and M.Á.G.; visualization, A.d.I.V. and C.G.; supervision, M.Á.G.; project administration, M.Á.G.; funding acquisition, M.Á.G. All authors have read and agreed to the published version of the manuscript.

Funding: This research was funded by the European Union’s Horizon 2020 research and innovation program under Grant Agreement No. 776661 (SOCLIMPACT project).

Acknowledgments: We are grateful to the reviewers for their insightful comments.

Conflicts of Interest: The authors declare no conflict of interest.

Appendix A



Figure A1. Mediterranean islands considered in the current study.

Appendix A.1. Calculation of N_c

Normalized values for projected ensemble mean changes for the selected energy indicators in the different regions, time periods and scenarios are given by the N_c index. The N_c index is defined in Equation (A1):

$$N_c = 0.25 \cdot A + 0.75 \cdot B \quad (\text{A1})$$

The terms A and B are individually normalized as follows:

A: To calculate it we first compute (for each indicator, time period and scenario), the absolute maximum ensemble mean increase (Δ_{\max}) and the absolute maximum ensemble mean decrease (Δ_{\min}) of all the islands. In the case of productivity, Δ_{\max} and Δ_{\min} are provided in kWh/kW. In the case of energy productivity droughts, Δ_{\max} and Δ_{\min} are given in absolute change (%).

Then, the ensemble mean change for a given region, time period and scenario (Δ_{mean}) is compared to the maximum change encountered for the corresponding case taking into account all islands. For the productivity case, Δ_{mean} is given in kWh/kW and for energy productivity droughts this is provided in absolute change (%). Specifically, if $\Delta_{\text{mean}} > 0$, Δ_{mean} is compared to Δ_{\max} . Alternatively, if $\Delta_{\text{mean}} < 0$, Δ_{mean} is compared to Δ_{\min} . In each case, the value of A is estimated with a linear regression as follows:

Wind and photovoltaic productivity:

Positive ensemble mean changes ($\Delta_{\text{mean}} > 0$), correspond to values of A from 0 to 0.5, whereas negative ensemble mean changes ($\Delta_{\text{mean}} < 0$) correspond to values of A from 0.5 to 1. To obtain the value of A within each interval, the following linear regression is applied:

$$\text{Positive ensemble mean changes: } A = ((-0.5 \cdot \Delta_{\text{mean}}) / (\Delta_{\max})) + 0.5 \quad (\text{A2})$$

$$\text{Negative ensemble mean changes: } A = ((0.5 \cdot \Delta_{\text{mean}}) / (\Delta_{\min})) + 0.5 \quad (\text{A3})$$

Wind and photovoltaic productivity droughts:

Positive ensemble mean changes in the frequency of productivity droughts ($\Delta_{\text{mean}} > 0$) correspond to values of A from 0.5 to 1, while negative ensemble mean changes ($\Delta_{\text{mean}} < 0$) correspond to values of A between 0 and 0.5. A is obtained as indicated in Equations (A4) and (A5):

$$\text{Positive ensemble mean changes: } A = ((0.5 \cdot \Delta_{\text{mean}}) / (\Delta_{\max})) + 0.5 \quad (\text{A4})$$

$$\text{Negative ensemble mean changes: } A = ((-0.5 \cdot \Delta_{\text{mean}}) / (\Delta_{\min})) + 0.5 \quad (\text{A5})$$

B: to compute it we express the relative ensemble mean change of the indicators with respect to the control time period in percentage ($\Delta_{\text{mean}_{\text{per}}}$) and compare it to a threshold of $\pm 10\%$. In the case of energy productivity droughts, $\Delta_{\text{mean}_{\text{per}}}$ gives the relative change (%). B is calculated with a linear regression as specified below:

Wind and photovoltaic productivity:

For productivity changes greater than 10% ($\Delta_{\text{mean}_{\text{per}}} \geq 10$) B is set to 0, whereas for productivity changes smaller than -10% ($\Delta_{\text{mean}_{\text{per}}} \leq -10$), the normalized value of B is 1. The normalized value of B , when changes range between -10% and 10% , is obtained with the following linear regression:

$$B = 1/20 \cdot (10 - \Delta_{\text{mean}_{\text{per}}}) \quad (\text{A6})$$

Energy productivity droughts:

Relative changes in the frequency of energy productivity greater than 10% ($\Delta_{\text{mean}_{\text{per}}} \geq 10$) correspond to a normalized B of 1. For relative changes in the occurrence of energy productivity

droughts smaller than -10% ($\Delta\text{mean}_{\text{per}} \leq -10$), the normalized value of B is 0. The normalized value of B is obtained with the linear regression shown in Equation (A7):

$$B = 1/20 \cdot (10 + \Delta\text{mean}_{\text{per}}) \tag{A7}$$

Appendix A.2. Calculation of Nu

Normalized uncertainties associated with ensemble mean projected changes for each island, scenario and time period are provided by Nu. This index is defined as follows:

$$\text{Nu} = (C \cdot 0.5) + (D \cdot 0.5) \tag{A8}$$

In this case,

$$C = \text{abs}((\text{ENSmin} - \text{ENSmax})/\Delta\text{mean}) \tag{A9}$$

where ENSmin and ENSmax correspond to the ensemble minimum and maximum changes with respect to the control, and Δmean is the ensemble mean change with respect to the control in each case. For productivity indicators, changes are in absolute terms (kWh/kW). In energy productivity droughts, ENSmin, ENSmax and Δmean are given in absolute change (%). Values of C greater than one are automatically set to 1. Values of C close to 0 indicate that ENSmin and ENSmax are close to Δmean and therefore that the spread of projected changes is small. Values of C close to one indicate a great spread in projected changes between the ensemble members.

The value of D depends on the sign of the ENSmin and ENSmax.

If ENSmin and ENSmax have the same sign: $D = 0$.

If ENSmin and ENSmax have a different sign: $D = 1$.

Appendix A.3. Tables with the Corresponding Values of Nu

Table A1. Normalized uncertainty (Nu) for wind productivity for each island, scenario and time period. Deep green cells: Nu = 0–0.2; Light green: Nu = 0.3–0.4; White: Nu = 0.5; Light yellow: Nu = 0.6–0.7; Deep yellow: Nu = 0.8–1. Nu is computed over land.

Wind Productivity (Land)		Balearic Islands	Corsica	Crete	Cyprus	Malta	Sardinia	Sicily
RCP2.6	2046–2065	0.5	0.5	0.2	1.0	0.5	0.5	1.0
	2081–2100	0.5	1.0	0.0	0.5	1.0	0.5	1.0
RCP8.5	2046–2065	0.2	1.0	1.0	1.0	1.0	1.0	1.0
	2081–2100	0.3	1.0	1.0	0.5	0.5	1.0	0.2

Table A2. This is equivalent to Table A1, but this is computed over the sea. Domains used to do the calculations are presented in Table 1.

Wind Productivity (Sea)		Balearic Islands	Corsica	Crete	Cyprus	Malta	Sardinia	Sicily
RCP2.6	2046–2065	0.2	1.0	0.4	1.0	0.3	1.0	0.3
	2081–2100	0.1	0.2	0.5	1.0	1.0	0.2	1.0
RCP8.5	2046–2065	0.3	1.0	1.0	0.5	0.5	1.0	0.5
	2081–2100	0.3	0.3	1.0	1.0	0.2	0.3	0.2

Table A3. Normalized uncertainty (Nu) for wind productivity droughts for each island, scenario and time period. Deep green cells: Nu = 0–0.2; Light green: Nu = 0.3–0.4; White: Nu = 0.5; Light yellow: Nu = 0.6–0.7; Deep yellow: Nu = 0.8–1. Nu is computed over land.

Wind Droughts		Balearic Islands	Corsica	Crete	Cyprus	Malta	Sardinia	Sicily
RCP2.6	2046–2065	0.3	1.0	0.5	1.0	0.4	0.5	1.0
	2081–2100	0.3	1.0	0.2	0.1	1.0	1.0	0.1
RCP8.5	2046–2065	0.3	0.5	1.0	0.5	0.5	0.5	0.5
	2081–2100	0.3	0.5	1.0	0.5	0.4	0.5	0.2

Table A4. Normalized uncertainty (Nu) for PV productivity for each island, scenario and time period. Deep green cells: Nu = 0–0.2; Light green: Nu = 0.3–0.4; White: Nu = 0.5; light yellow: Nu = 0.6–0.7; Deep yellow: Nu = 0.8–1. Nu is computed over land.

PV Productivity (Land)		Balearic Islands	Corsica	Crete	Cyprus	Malta	Sardinia	Sicily
RCP2.6	2046–2065	1.0	0.5	1.0	1.0	0.5	0.5	0.5
	2081–2100	1.0	1.0	1.0	0.0	1.0	1.0	1.0
RCP8.5	2046–2065	0.5	0.4	0.5	0.5	0.5	1.0	0.5
	2081–2100	0.5	0.5	1.0	0.5	0.4	0.5	0.5

Table A5. This is equivalent to Table A4, but this is computed over the sea. Domains used to do the calculations are presented in Table 1.

PV Productivity (Sea)		Balearic Islands	Corsica	Crete	Cyprus	Malta	Sardinia	Sicily
RCP2.6	2046–2065	0.1	0.4	0.5	0.2	0.2	0.4	0.2
	2081–2100	0.5	0.5	0.4	0.0	0.5	0.5	0.5
RCP8.5	2046–2065	0.4	0.4	0.3	0.4	0.4	0.4	0.4
	2081–2100	0.3	0.3	0.2	0.3	0.2	0.3	0.2

Table A6. Normalized uncertainty (Nu) for PV productivity droughts for each island, scenario and time period. Deep green cells: Nu = 0–0.2; Light green: Nu = 0.3–0.4; White: Nu = 0.5; Light yellow: Nu = 0.6–0.7; Deep yellow: Nu = 0.8–1. Nu is computed over land.

PV Droughts		Balearic Islands	Corsica	Crete	Cyprus	Malta	Sardinia	Sicily
RCP2.6	2046–2065	0.5	1.0	0.4	1.0	1.0	0.5	0.1
	2081–2100	1.0	1.0	0.1	0.4	1.0	1.0	1.0
RCP8.5	2046–2065	1.0	1.0	1.0	0.5	1.0	1.0	1.0
	2081–2100	1.0	0.5	1.0	0.5	1.0	0.5	0.5

References

1. Giorgi, F. Climate Change Hot-Spots. *Geophys. Res. Lett.* **2006**, *33*. [CrossRef]
2. Marcinkowski, H.M.; Alberg Østergaard, P.; Roth Djørup, S. Transitioning Island Energy Systems—Local Conditions, Development Phases, and Renewable Energy Integration. *Energies* **2019**, *12*, 3484. [CrossRef]
3. Kougiyas, I.; Szabó, S.; Nikitas, A.; Theodossiou, N. Sustainable Energy Modelling of Non-Interconnected Mediterranean Islands. *Renew. Energy* **2019**, *133*, 930–940. [CrossRef]
4. Political Declaration on Clean Energy for Eu Islands. Available online: https://ec.europa.eu/energy/sites/ener/files/documents/170505_political_declaration_on_clean_energy_for_eu_islands-final_version_16_05_20171.pdf (accessed on 16 September 2020).
5. Lacerda, J.S.; Van den Bergh, J.C.J.M. International Diffusion of Renewable Energy Innovations: Lessons from the Lead Markets for Wind Power in China, Germany and USA. *Energies* **2014**, *7*, 8236–8263. [CrossRef]
6. Busu, M. Measuring the Renewable Energy Efficiency at the European Union Level and Its Impact on CO₂ Emissions. *Processes* **2019**, *7*, 923. [CrossRef]

7. Tobin, I.; Vautard, R.; Balog, I.; Bréon, F.-M.; Jerez, S.; Ruti, P.M.; Thais, F.; Vrac, M.; Yiou, P. Assessing Climate Change Impacts on European Wind Energy from ENSEMBLES High-Resolution Climate Projections. *Clim. Chang.* **2015**, *128*, 99–112. [[CrossRef](#)]
8. Tobin, I.; Jerez, S.; Vautard, R.; Thais, F.; van Meijgaard, E.; Prein, A.; Déqué, M.; Kotlarski, S.; Maule, C.F.; Nikulin, G.; et al. Climate Change Impacts on the Power Generation Potential of a European Mid-Century Wind Farms Scenario. *Environ. Res. Lett.* **2016**, *11*, 034013. [[CrossRef](#)]
9. Jerez, S.; Tobin, I.; Vautard, R.; Montávez, J.P.; López-Romero, J.M.; Thais, F.; Bartok, B.; Christensen, O.B.; Colette, A.; Déqué, M.; et al. The Impact of Climate Change on Photovoltaic Power Generation in Europe. *Nat. Commun.* **2015**, *6*, 1–8. [[CrossRef](#)]
10. Jerez, S.; Thais, F.; Tobin, I.; Wild, M.; Colette, A.; Yiou, P.; Vautard, R. The CLIMIX Model: A Tool to Create and Evaluate Spatially-Resolved Scenarios of Photovoltaic and Wind Power Development. *Renew. Sustain. Energy Rev.* **2015**, *42*, 1–15. [[CrossRef](#)]
11. Panagea, I.S.; Tsanis, I.K.; Koutroulis, A.G.; Grillakis, M.G. Climate Change Impact on Photovoltaic Energy Output: The Case of Greece. Available online: <https://www.hindawi.com/journals/amete/2014/264506/> (accessed on 24 March 2020). [[CrossRef](#)]
12. Crook, J.A.; Jones, L.A.; Forster, P.M.; Crook, R. Climate Change Impacts on Future Photovoltaic and Concentrated Solar Power Energy Output. *Energy Environ. Sci.* **2011**, *4*, 3101–3109. [[CrossRef](#)]
13. Wild, M.; Folini, D.; Henschel, F.; Fischer, N.; Müller, B. Projections of Long-Term Changes in Solar Radiation Based on CMIP5 Climate Models and Their Influence on Energy Yields of Photovoltaic Systems. *Sol. Energy* **2015**, *116*, 12–24. [[CrossRef](#)]
14. Gil, V.; Gaertner, M.A.; Gutierrez, C.; Losada, T. Impact of Climate Change on Solar Irradiation and Variability over the Iberian Peninsula Using Regional Climate Models. *Int. J. Climatol.* **2019**, *39*, 1733–1747. [[CrossRef](#)]
15. Gutiérrez, C.; Somot, S.; Nabat, P.; Mallet, M.; Corre, L.; van Meijgaard, E.; Perpiñán, O.; Gaertner, M.Á. Future Evolution of Surface Solar Radiation and Photovoltaic Potential in Europe: Investigating the Role of Aerosols. *Environ. Res. Lett.* **2020**, *15*, 034035. [[CrossRef](#)]
16. Jerez, S.; Tobin, I.; Turco, M.; Jiménez-Guerrero, P.; Vautard, R.; Montávez, J.P. Future Changes, or Lack Thereof, in the Temporal Variability of the Combined Wind-Plus-Solar Power Production in Europe. *Renew. Energy* **2019**, *139*, 251–260. [[CrossRef](#)]
17. Boé, J.; Somot, S.; Corre, L.; Nabat, P. Large Discrepancies in Summer Climate Change over Europe as Projected by Global and Regional Climate Models: Causes and Consequences. *Clim. Dyn.* **2020**, *54*, 2981–3002. [[CrossRef](#)]
18. Jacob, D.; Teichmann, C.; Sobolowski, S.; Katragkou, E.; Anders, I.; Belda, M.; Benestad, R.; Boberg, F.; Buonomo, E.; Cardoso, R.M.; et al. Regional climate downscaling over Europe: Perspectives from the EURO-CORDEX community. *Reg. Environ. Chang.* **2020**, *20*. [[CrossRef](#)]
19. Pantusa, D.; Tomasicchio, G.R. Large-Scale Offshore Wind Production in the Mediterranean Sea. *Cogent Eng.* **2019**, *6*, 1661112. [[CrossRef](#)]
20. Global Wind Energy Council. *Global Offshore Wind Report 2020*; Global Wind Energy Council: Brussels, Belgium, 2020; Available online: <https://gwec.net/global-offshore-wind-report-2020/> (accessed on 24 September 2020).
21. Abanades, J. Wind Energy in the Mediterranean Spanish ARC: The Application of Gravity Based Solutions. *Front. Energy Res.* **2019**, *7*. [[CrossRef](#)]
22. WindEurope. *Offshore Wind in Europe—Key Trends and Statistics 2019*. 2020. Available online: <https://windeurope.org/wp-content/uploads/files/about-wind/statistics/WindEurope-Annual-Offshore-Statistics-2019.pdf> (accessed on 24 September 2020).
23. Newly Installed Dutch Offshore Solar Farm Survives First Storms|SWZ|Maritime. Available online: <https://www.swzmaritime.nl/news/2019/12/12/newly-installed-dutch-offshore-solar-farm-survives-first-storms/> (accessed on 2 April 2020).
24. Witzke, U.; Cadamuro, M.; Aquilina, M.; Mule' Stagno, L.; Grech, M. Floating Photovoltaic Installations in the Maltese Sea Waters. In Proceedings of the 32nd European Photovoltaic Solar Energy Conference and Exhibition, Munich, Germany, 20–24 June 2016; pp. 1964–1968. [[CrossRef](#)]
25. Trapani, K.; Millar, D.L.; Smith, H.C.M. Novel Offshore Application of Photovoltaics in Comparison to Conventional Marine Renewable Energy Technologies. *Renew. Energy* **2013**, *50*, 879–888. [[CrossRef](#)]

26. Khalilian, S.; Shahvari, N.A. SWAT Evaluation of the Effects of Climate Change on Renewable Water Resources in Salt Lake Sub-Basin, Iran. *AgriEngineering* **2019**, *1*, 44–57. [[CrossRef](#)]
27. Ocean Energy Europe. Ocean Energy Key Trends and Statistics 2019; 2020. Available online: https://www.oceanenergy-europe.eu/wp-content/uploads/2020/03/OEE_Trends-Stats_2019_Web.pdf (accessed on 24 September 2020).
28. Golroodbari, S.Z.; van Sark, W. Simulation of Performance Differences between Offshore and Land-Based Photovoltaic Systems. *Prog. Photovolt. Res. Appl.* **2020**, *28*, 873–886. [[CrossRef](#)]
29. Alvarez, I.; Lorenzo, M.N. Changes in Offshore Wind Power Potential over the Mediterranean Sea Using CORDEX Projections. *Reg. Environ. Chang.* **2019**, *19*, 79–88. [[CrossRef](#)]
30. Koletsis, I.; Kotroni, V.; Lagouvardos, K.; Soukissian, T. Assessment of Offshore Wind Speed and Power Potential over the Mediterranean and the Black Seas under Future Climate Changes. *Renew. Sustain. Energy Rev.* **2016**, *60*, 234–245. [[CrossRef](#)]
31. Moss, R.H.; Babiker, W.; Brinkman, S.; Calvo, E.; Carter, T.; Edmonds, J.; Elgizouli, I.; Emori, S.; Erda, L.; Hibbard, K.; et al. *Towards New Scenarios for Analysis of Emissions, Climate Change, Impacts, and Response Strategies*; IPCC Expert Meeting Report on new scenarios; IPCC: Geneva, Switzerland, 2008; Available online: <https://archive.ipcc.ch/pdf/supporting-material/expert-meeting-report-scenarios.pdf> (accessed on 24 September 2020).
32. Raynaud, D.; Hingray, B.; François, B.; Creutin, J.D. Energy Droughts from Variable Renewable Energy Sources in European Climates. *Renew. Energy* **2018**, *125*, 578–589. [[CrossRef](#)]
33. Déqué, M.; Rowell, D.P.; Lüthi, D.; Giorgi, F.; Christensen, J.H.; Rockel, B.; Jacob, D.; Kjellström, E.; de Castro, M.; van den Hurk, B. An Intercomparison of Regional Climate Simulations for Europe: Assessing Uncertainties in Model Projections. *Clim. Chang.* **2007**, *81*, 53–70. [[CrossRef](#)]
34. McSweeney, C.F.; Jones, R.G.; Lee, R.W.; Rowell, D.P. Selecting CMIP5 GCMs for downscaling over multiple regions. *Clim. Dyn.* **2015**, *44*, 3237–3260. [[CrossRef](#)]
35. Gutiérrez, C.; Somot, S.; Nabat, P.; Mallet, M.; Gaertner, M.Á.; Perpiñán, O. Impact of Aerosols on the Spatiotemporal Variability of Photovoltaic Energy Production in the Euro-Mediterranean Area. *Sol. Energy* **2018**, *174*, 1142–1152. [[CrossRef](#)]
36. Perpiñán, O. Statistical Analysis of the Performance and Simulation of a Two-Axis Tracking PV System. *Sol. Energy* **2009**, *83*, 2074–2085. [[CrossRef](#)]
37. Gutiérrez, C.; Gaertner, M.Á.; Perpiñán, O.; Gallardo, C.; Sánchez, E. A Multi-Step Scheme for Spatial Analysis of Solar and Photovoltaic Production Variability and Complementarity. *Sol. Energy* **2017**, *158*, 100–116. [[CrossRef](#)]
38. Devis, A.; Lipzig, N.P.M.V.; Demuzere, M. Should Future Wind Speed Changes Be Taken into Account in Wind Farm Development? *Environ. Res. Lett.* **2018**, *13*, 064012. [[CrossRef](#)]
39. Solaun, K.; Cerdá, E. Climate Change Impacts on Renewable Energy Generation. A Review of Quantitative Projections. *Renew. Sustain. Energy Rev.* **2019**, *116*, 109415. [[CrossRef](#)]
40. Solaun, K.; Cerdá, E. Impacts of Climate Change on Wind Energy Power—Four Wind Farms in Spain. *Renew. Energy* **2020**, *145*, 1306–1316. [[CrossRef](#)]
41. Šuri, M.; Huld, T.A.; Dunlop, E.D.; Ossenbrink, H.A. Potential of Solar Electricity Generation in the European Union Member States and Candidate Countries. *Sol. Energy* **2007**, *81*, 1295–1305. [[CrossRef](#)]
42. Huld, T.; Müller, R.; Gambardella, A. A New Solar Radiation Database for Estimating PV Performance in Europe and Africa. *Sol. Energy* **2012**, *86*, 1803–1815. [[CrossRef](#)]
43. Gérégnny, O.; Coudray, S.; Lapucci, C.; Tomasino, C.; Bisgambiglia, P.-A.; Galgani, F. Small-Scale Variability of the Current in the Strait of Bonifacio. *Ocean Dyn.* **2015**, *65*, 1165–1182. [[CrossRef](#)]
44. Deloitte Spain. Los Territorios no Peninsulares 100% descarbonizados en 2040. Available online: <https://www2.deloitte.com/es/es/pages/strategy/articles/territorios-no-peninsulares-descarbonizados-2040.html> (accessed on 24 August 2020).
45. Pisacane, G.; Sannino, G.; Carillo, A.; Struglia, M.V.; Bastianoni, S. Marine energy exploitation in the mediterranean region: Steps forward and challenges. *Front. Energy Res.* **2019**, *6*, 109. [[CrossRef](#)]

46. WavEC: Combined Wind, Wave and Solar to Transform Marine Energy. Available online: <https://marineenergy.biz/2019/12/16/wavec-combined-wind-wave-and-solar-to-transform-marine-energy/> (accessed on 16 September 2020).
47. MaREI to Lead €9m Project to Build Floating Offshore Platform. Available online: <https://www.marei.ie/marei-to-lead-e9m-project-to-build-floating-offshore-platform/> (accessed on 16 September 2020).



© 2020 by the authors. Licensee MDPI, Basel, Switzerland. This article is an open access article distributed under the terms and conditions of the Creative Commons Attribution (CC BY) license (<http://creativecommons.org/licenses/by/4.0/>).